



# Cr(VI) removal from aqueous solution using *Psidium guajava* leaves as green adsorbent: column studies

Tania Mitra<sup>1</sup> · Sudip Kumar Das<sup>1</sup>

Received: 7 November 2018 / Accepted: 31 July 2019 / Published online: 22 August 2019  
© The Author(s) 2019

## Abstract

This paper deals with the experimental investigation of the removal of the toxic Cr(VI) ions using a low-cost waste biomaterials *Psidium guajava* leaves as the adsorbent in continuous column mode. The influence of process parameters like bed depth, the rate of flow, and influent concentration on the removal was investigated to determine the adsorption characteristics by this adsorbent. The capacity of the adsorbent for metal uptake was decreased with the increase in bed depth from 4.07 to 2.89 mg g<sup>-1</sup>, but it was increased with the rise in flow rate from 2.94 to 8.72 mg g<sup>-1</sup>. The data obtained from the experiment were fitted good with Thomas model. The major functional groups were identified from the FTIR study which was responsible for the adsorption. The guava leaves are suitable for Cr(VI) removal from aqueous solution.

**Keywords** Guava leaves · Green adsorbent · Fixed-bed · Thomas model · Bohart–Adams model

## List of symbols

$C_{ad}$	Adsorbed concentration (mg L <sup>-1</sup> )
$C_0$	Influent metal ion concentration at $t = 0$ (mg L <sup>-1</sup> )
$C_t$	Affluent metal ion concentration at time $t$ (mg L <sup>-1</sup> )
$C_t/C_0$	Relative concentration
$C_w$	Concentration of Cr(VI) in wastewater (mg L <sup>-1</sup> )
$D$	Diameter of the column (cm)
$H$	Total height of the column (cm)
$H_c$	Additional height for the column accessories (cm)
$H_U$	The length of bed used to breakthrough point (cm)
$H_{UNU}$	The length of bed unused (cm)
$K_{AB}$	Kinetic constant for Bohart–Adams model (L mg <sup>-1</sup> )
$k_{th}$	Thomas rate constant (L mg <sup>-1</sup> min <sup>-1</sup> )
$N_0$	Saturation concentration (mg L <sup>-1</sup> )
$q$	Adsorption capacity (mg g <sup>-1</sup> )
$M_{ad}$	Amount of adsorbent in the designed tower (g)
$q_0$	Maximum metal uptake per gram of the adsorbent (mg g <sup>-1</sup> )
$q_{eq}$	Equilibrium metal uptake by adsorbent (mg g <sup>-1</sup> )
$q_{max}$	Maximum adsorption capacity of the adsorbent (mg g <sup>-1</sup> )
$q_t$	Total adsorbed Cr(VI) at time $t$ (mg)

$q_{t0}$	Total adsorbed Cr(VI) at time $t = 0$ (mg)
$Q_d$	Volumetric flow rate at designed column (mL min <sup>-1</sup> )
$R^2$	Correlation coefficient
$t_b$	Breakthrough time (min)
$t_R$	Regeneration time (min)
$t_t$	Time equilibrium to stoichiometric capacity (min)
$t_u$	Time equivalent to the usable capacity (min)
$T$	Total working time (h)
$u_0$	Superficial velocity (m min <sup>-1</sup> )
$V_{eff}$	Affluent volume (mL)
$x$	Amount of adsorbent present in the column (g)
$Z$	Bed depth (cm)

## Greek symbols

$v$	Flow rate (mL min <sup>-1</sup> )
$\rho$	Density of the adsorbent (kg m <sup>3</sup> )

## Introduction

The environmentalists are very much concern for the heavy metal ions which are present in the water stream which throws a serious threat to human health and also the environment as they are not biodegradable and toxic (Sousa et al. 2010; Long et al. 2014). So, the most important environmental issue for recent time is the removal of the toxic heavy metals from the wastewater (Mondal 2009). The metals having the atomic density greater than 4 g cm<sup>-3</sup> are termed as heavy metals

✉ Sudip Kumar Das  
drsudipkdas@vsnl.net; skdchemengg@caluniv.ac.in

<sup>1</sup> Department of Chemical Engineering, University of Calcutta, 92, A. P. C. Road, Kolkata 700 009, India

(Uguzdogan et al. 2010; Kalhori et al. 2013). Among them, hexavalent chromium is known worldwide as a carcinogenic heavy metal with other harmful effects on human health including skin allergy, liver, and pulmonary damage (Dakiky et al. 2002; Setshedi et al. 2015). Cr(VI) ion is released into the aquatic environment from the variety of sources such as electroplating industries, wood preservation, leather tanning, and metal finishing industries (Quintelas et al. 2009; Ye et al. 2010). The international standards like EPA, IS, and WHO set the discharge limit of Cr(VI) ion limit such industries to the environment. These limits are  $0.1 \text{ mg L}^{-1}$  for EPA,  $0.1 \text{ mg L}^{-1}$  for IS, and  $0.05 \text{ mg L}^{-1}$  for WHO, respectively (EPA 1990; IS 1050; WHO 1993). Conventional methods, like chemical precipitation, ion exchange, reverse osmosis, extraction, membrane separation, adsorption using activated carbon, biosorption, etc., are used for the removal of heavy metals from aqueous solution (Ye et al. 2010; Alguacil et al. 2008). Among them, reverse osmosis and membrane separation are too much expensive due to the cost of the membrane. Ion exchange, precipitation, and extraction cannot give the satisfactory result, but the processes are not very effective and also a large amount of sludge formation. Adsorption using activated carbon is also not a cost-effective process due to its high initial cost, and also the regeneration cost is too high. All the methods mentioned above except adsorption are costly and also not eco-friendly. Biosorption is an economically cheap process if low-cost waste materials are identified as adsorbents which require an easy operation method (Mitra et al. 2014; Agarwal et al. 2006). Researchers used coconut shell, fly ash, neem leaves, hyacinth root, sawdust, rice husk, rice straw, rice bran, rubber leaf powder, onion peel, mango and bamboo leaf, etc., as green adsorbents for Cr(VI) ion removal from wastewater (Singha et al. 2011; Nag et al. 2017). Hence, a lot of research works are needed with the low-cost, easily available adsorbent to remove or to reduce this environmental problem (Agarwal et al. 2006). *Psidium guajava* (guava) is a traditional medicinal plant. It is a native of Central America but is now widely cultivated more than fifty countries particularly in tropics, subtropics, and some of the Mediterranean areas. The major cultivators in the world are India, Brazil, and Mexico. South Africa, Jamaica, Kenya, Cuba, the USA (Mainly Florida and Hawaii), Egypt, Columbia, and the Philippines, etc., are the other leading guava producing countries (Shruthi et al. 2013; Hossen 2012). Guava leaves are waste materials and can be used for this process which makes the process economical.

In this study, the adsorbent is introduced as the green adsorbent. The primary sources of green adsorbents are the waste of fruits, vegetables, trees, the bark of the trees and agricultural, bi-products of agricultural waste, etc. These are low cost compared to the treated or modified complex adsorbents. The capacity of these adsorbents is less than the complex adsorbents but cost-potentiality makes the use of green adsorbents greater and competitive (Kyzas and Kostoglou 2014).

The present study deals with the fixed-bed adsorption using guava leaves for Cr(VI) ion removal. The variation of process parameters, like influent concentration, flow rate, bed depth, adsorbent dose, etc., will be carried out. Mathematical modeling for column mode will be performed in this study.

## Materials and methods

Guava leaves were collected from guava trees from Kolkata, West Bengal, India. These were washed for several times and dried under the sun for 6–7 days. They were then dried in the oven at  $70 \text{ }^\circ\text{C}$  for 8–9 h and crushed and sieved to get particle sizes of 290–350  $\mu\text{m}$ .

Stock solution of  $1000 \text{ mg L}^{-1}$  Cr(VI) was prepared by dissolving 2.829 gm  $\text{K}_2\text{Cr}_2\text{O}_7$  of in distilled water. All the chemicals used are manufactured by E. Merck India Pvt. Ltd. (Mumbai). Pump (Cole-Parmer, model-73 7535-04, USA) was helped to flow the Cr(VI) ion solution to the column. All other instruments used in this study were same as our earlier column experiment (Mitra and Das 2016).

## Experimental

### Column study

The columns are made of glass of length 50 cm, and the internal diameter of 1.8 cm was used for these experiments (Fig. 1). A metal sieve plate was placed at the bottom of the column, and glass wool was placed above the sieve plate as the preventing measure from the loss of adsorbents to prepare desired bed height. After adding the adsorbent to the column, the distilled water was to be added to make the bed of fixed height. The downward flow of metal ion solution was carried out by using the multichannel peristaltic pump, and from bottom samples were collected at the desired interval of time for Cr(VI) analysis.

## Results and discussion

The plot of relative concentration ( $C/C_0$ ) versus contact time was used to explain the column performance. Total adsorbed metal ion for a particular flow rate was evaluated by using the following equation,

$$q_t = \frac{v}{1000} \int_{t_0}^{t_s} C_{\text{ad}} dt \quad (1)$$

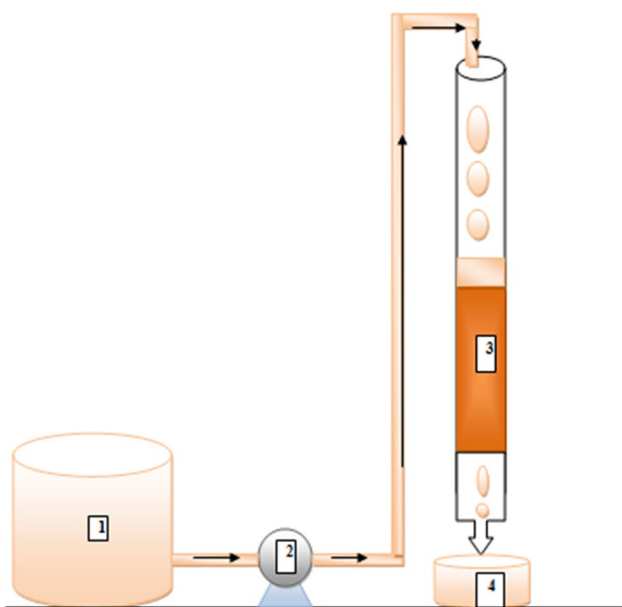


**Fig. 1** Schematic diagram of column process. 1. Feed storage; 2. Pump; 3. Fixed-bed (adsorbent); 4. Effluent

The equilibrium metal ion uptake was determined using the following equation which is dependent on the weight of the adsorbent,

$$q_{eq} = \frac{q_t - q_{t0}}{x} \tag{2}$$

The height of the mass transfer zone depends on several parameters like flow rate, the rate of mass transfer, and diffusion in pores. Several theoretical predictions had been done to predict the mass transfer zone but some uncertainties in flow pattern make it inaccurate. Hence, it is necessary to experiment in a laboratory scale to scale up the results.

The stoichiometric capacity of the adsorbent used in the bed is determined as follows,

$$t_t = \int_0^{\alpha} \left(1 - \frac{C_t}{C_0}\right) dt \tag{3}$$

The usable capacity of the adsorbent up to breakthrough time ( $t_b$ ) is given by the following equation,

$$t_u = \int_0^{t_b} \left(1 - \frac{C_t}{C_0}\right) dt \tag{4}$$

The length of the bed used to the breakthrough point is calculated as,

$$H_U = \frac{t_u}{t_t} Z \tag{5}$$

The unused bed length is the remaining fraction times the total height of the bed, as

$$H_{UNU} = \left(1 - \frac{t_u}{t_t}\right) Z \tag{6}$$

### Characteristics of the adsorbent

The physical characteristics of guava leaves were presented in Table 1. Figure 2 represents the photograph of SEM and shows the surface morphology of the raw guava leaves. Function groups present in the unloaded and metal ion-loaded guava leaf is identified by Fourier transform infrared spectra (FTIR) (Fig. 3).

### Influence of bed depth

Figure 4 shows the variation of bed depth (4–6 cm). As the increase in bed depth, both the saturation and exhaustion times were increased because more binding sites were available for adsorption. A larger mass transfer zone was found in the greater bed depth. The breakthrough curve characterized by an S-shape whose last part indicated a saturation zone for the process (Mitra and Das 2016).

**Table 1** Characteristics of guava leaves

Name of the adsorbent	Guava leaves
Particle size	290–350 $\mu\text{m}$
Surface area	7.7 $\text{m}^2 \text{g}^{-1}$
Point of zero charge	6.05

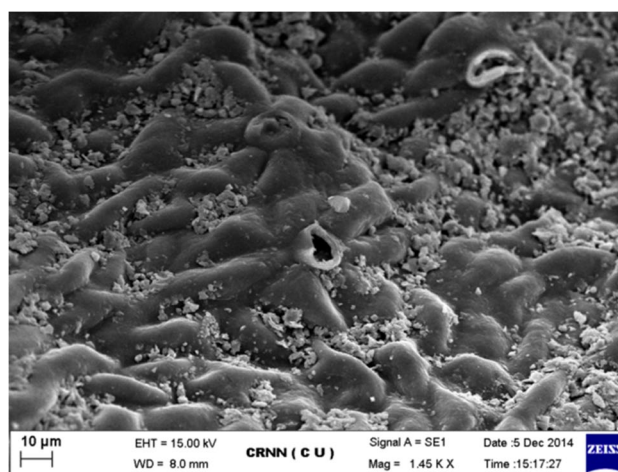


**Fig. 2** Scanning electron micrograph of guava leaves

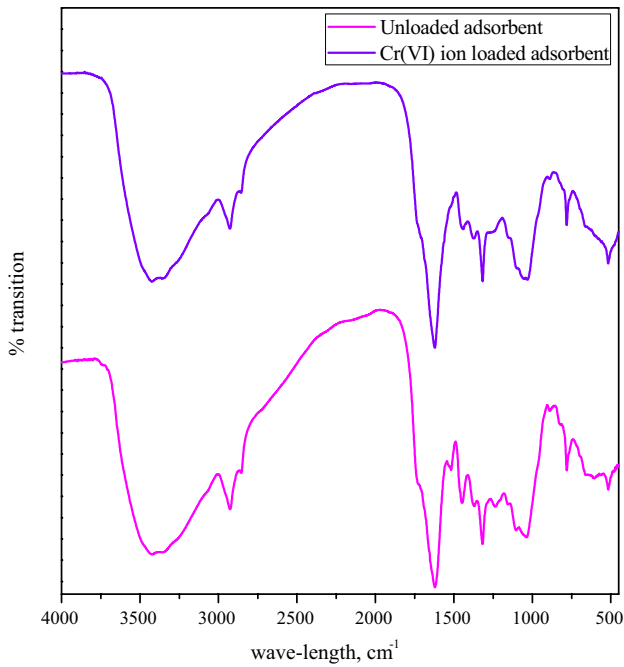


Fig. 3 FTIR plot for Cr(VI) ion adsorption using guava leaves

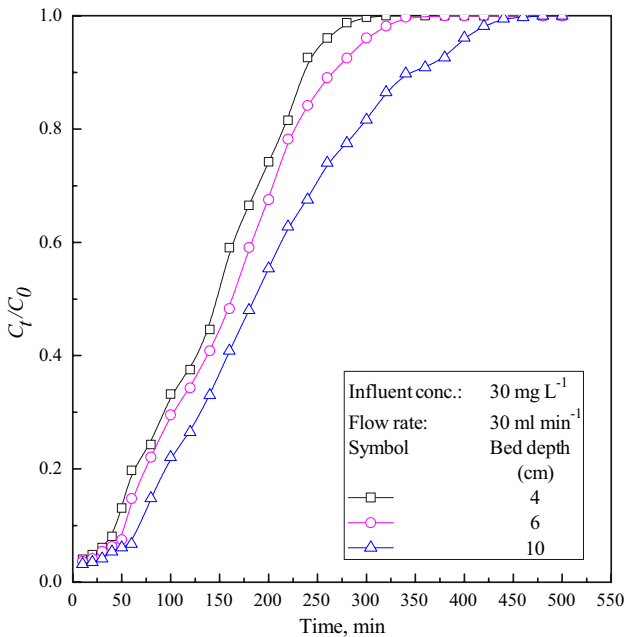


Fig. 4 Effect of bed depth for Cr(VI) ion adsorption

**Variation of flow rate**

The variation of different flows rate was shown in Fig. 5. At lower flow rates, the adsorption was very fast as the vacant adsorption sites are more available in the first stage. Gradually, it is decreased in the later stage as the occupancy of those sites

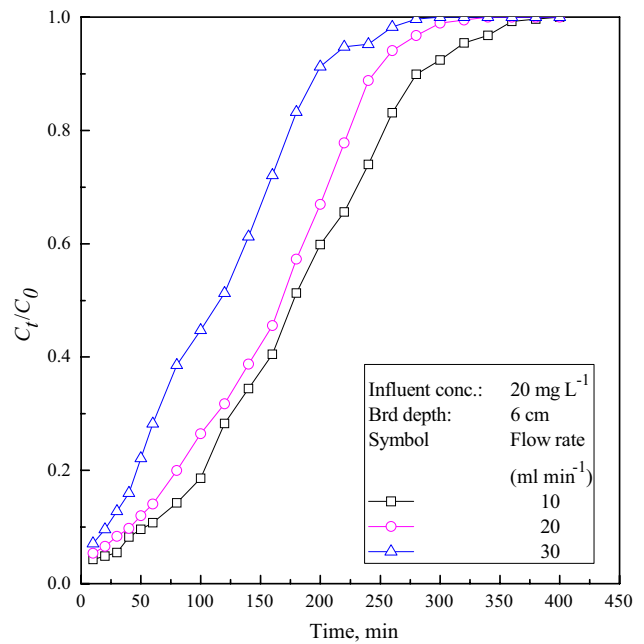


Fig. 5 Effect of flow rate for Cr(VI) ion adsorption

by metal ions, and the process becomes less efficient. Figure 5 shows a steeper breakthrough and exhaustion with the increase in the flow rates from 10 to 30 mg L<sup>-1</sup>. At lower flow rate, the best adsorption performance attained (Kalavathy et al. 2010).

**Influence of inlet concentration**

Figure 6 shows the variation of inlet concentration. As the increase in influent concentration, the breakthrough time decreased and is due to the rise of mass transfer driving force which resulted from the decrease in the mass transfer zone. It also makes an impact on metal uptake capacity. The uptake capacity decreases with the increase in inlet concentration (Talreja et al. 2014).

**Modeling of the column experiment**

The laboratory-scale column data need to analyze for developing it in the industrial system. The development of these data is made using well-known kinetic models (Setshedi et al. 2015).

**Thomas model (Thomas 1948)**

It is a widely used model to explain the performance of the adsorbent in the column study. Based on the Langmuir isotherm theory of sorption, and assumed the second-order reversible reaction kinetics. The model equation is,

$$\ln \left( \frac{C_0}{C_t} - 1 \right) = \frac{k_m q_0 x}{v} - k_{th} C_0 t \tag{7}$$

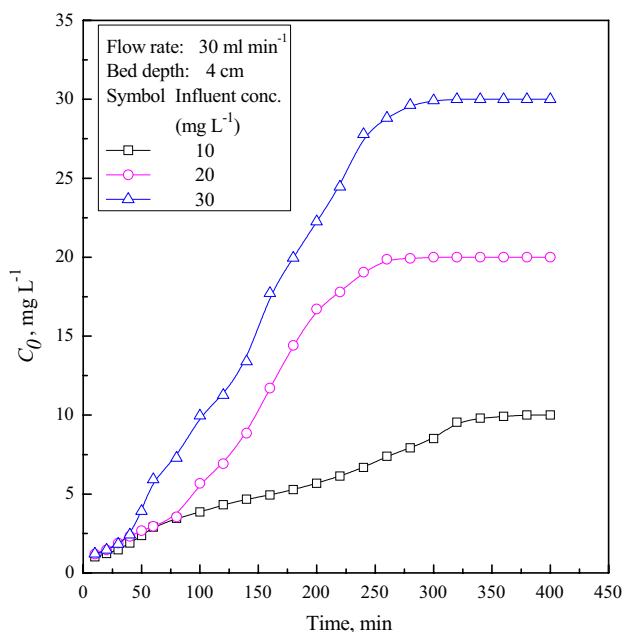


**Fig. 6** Effect of influent metal ion concentration for Cr(VI) ion adsorption

The rate constant of the Thomas model and metal uptake capacity was obtained from the plot of  $\ln[C_0/C_t - 1]$  versus  $t$  for the above equation and presented in Table 2. The  $k_{th}$  value was decreased, and  $q_0$  was increased with the increase in influent concentration.

**Bohart–Adams modell (Bohart and Adams 1920)**

The empirical model is Bohart–Adams model to design the column process. The surface reaction theory is the basis of this model and applicable in the first part in the breakthrough curve. The primary assumption is the adsorption rate is proportional to adsorption capacity. The linearized form of this equation is,

$$\ln \left( \frac{C_t}{C_0} \right) = K_{AB} C_0 t - K_{AB} N_0 \frac{z}{u_0} \tag{8}$$

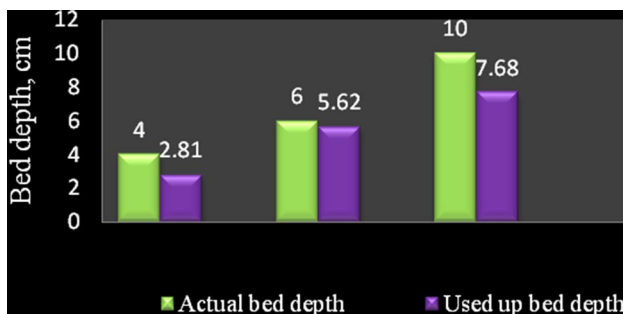
The model rate constant and saturation concentration were determined along with the correlation coefficient from the graph of  $\ln[C_t/C_0]$  versus  $t$  which is represented in Table 3. A decreasing trend was followed in the case of saturation concentration with the increased bed depth and flow rate, but the opposite trend was observed in the case of influent concentration. These trends strongly proved the influence

**Table 2** Model parameter for Thomas model

Variation of bed depth				
Influent concentration: 10 mg L <sup>-1</sup> ; flow rate: 10 mL min <sup>-1</sup>				
Bed depth Z (cm)	Equilibrium metal uptake $q_{eq}$ (mg g <sup>-1</sup> )	Rate constant $k_{th} \times 10^3$ (L mg <sup>-1</sup> min <sup>-1</sup> )	Maximum metal uptake $q_0$ (mg g <sup>-1</sup> )	Correlation coefficient ( $R^2$ )
4	4.07	2.906	3.299	0.9327
6	3.52	3.109	2.701	0.9935
10	2.89	1.518	3.146	0.9812
Variation of flow rate				
Influent concentration: 20 mg L <sup>-1</sup> ; bed depth: 10 cm				
Flow rate $v$ (mL min <sup>-1</sup> )	Equilibrium metal uptake $q_{eq}$ (mg g <sup>-1</sup> )	Rate constant $k_{th} \times 10^3$ (L mg <sup>-1</sup> min <sup>-1</sup> )	Maximum metal uptake $q_0$ (mg g <sup>-1</sup> )	Correlation coefficient ( $R^2$ )
10	2.94	0.872	6.74	0.9889
30	7.06	0.881	18.08	0.9864
40	8.72	1.227	15.96	0.9867
Variation of influent concentration				
Bed depth: 4 cm; flow rate: 10 mL min <sup>-1</sup>				
Influent concentration $C_0$ (mg L <sup>-1</sup> )	Equilibrium metal uptake $q_{eq}$ (mg g <sup>-1</sup> )	Rate constant $k_{th} \times 10^3$ (L mg <sup>-1</sup> min <sup>-1</sup> )	Maximum metal uptake $q_0$ (mg g <sup>-1</sup> )	Correlation coefficient ( $R^2$ )
10	4.07	2.906	3.299	0.9327
20	6.10	1.105	11.40	0.9843
30	5.99	0.767	18.32	0.9939

**Table 3** Model parameters for Bohart–Adams model

Variation of bed depth			
Influent concentration: 10 mg L <sup>-1</sup> ; flow rate: 10 mL min <sup>-1</sup>			
Bed depth Z (cm)	Rate constant $K_{AB} \times 10^3$ (L mg <sup>-1</sup> )	Saturation concentration $N_0$ (g L <sup>-1</sup> )	Correlation coefficient ( $R^2$ )
4	0.955	26.37	0.8276
6	0.996	18.92	0.8640
10	0.831	16.08	0.9288
Variation of flow rate			
Influent concentration: 20 mg L <sup>-1</sup> ; bed depth: 10 cm			
Flow rate $v$ (mL min <sup>-1</sup> )	Rate constant $K_{AB} \times 10^3$ (L mg <sup>-1</sup> )	Saturation concentration $N_0$ (g L <sup>-1</sup> )	Correlation coefficient ( $R^2$ )
10	0.670	26.09	0.9825
30	0.660	24.08	0.9746
40	0.670	19.27	0.9192
Variation of influent concentration			
Bed depth: 4 cm; flow rate: 10 mL min <sup>-1</sup>			
Influent concentration $C_0$ (mg L <sup>-1</sup> )	Rate constant $K_{AB} \times 10^3$ (L mg <sup>-1</sup> )	Saturation concentration $N_0$ (g L <sup>-1</sup> )	Correlation coefficient ( $R^2$ )
10	0.955	26.37	0.8276
20	0.830	47.60	0.9703
30	0.640	69.91	0.9923

**Fig. 7** Mass transfer zone

of external mass transfer to the sorption process (Malkoc et al. 2006).

### Determination of mass transfer zone (Geankoplis et al. 2016)

Using the above Eqs. (3–6), we determined the amount of adsorbent that had been used for the study. From Fig. 7, it is clear that not the whole bed is used for the adsorption process. Although the required bed height was 4 cm, 6 cm,

and 10 cm, little amount of adsorbent remain unused. This is because channeling in the bed occurred.

### Scale-up design for industrial use

Laboratory testing was done to initialize the industrial scale setup and optimize the adsorption capacity. The best condition used to design the setup in industrial purpose is determined from the best fitted kinetic model.

The volumetric rate of flow for the industrial designed setup is given as below,

$$Q_d = \frac{\pi D^2 u_0}{4} \quad (9)$$

here,  $D$  can be represented as,

$$D = \sqrt{\frac{4W}{\pi T u_0}} \quad (10)$$

The amount of guava leaves is used to design the process setup in industrial scale is determined using the following equation,

**Table 4** Functional group for FTIR analysis

Functional group	Unloaded adsorbent	Loaded adsorbent
Alkyl C–H stretching	2931	2927
Aromatic C=C bending	1623	1619
Carboxylate anion C=O stretching	1456	1445
–SO <sub>3</sub> stretching	1240	1236
Alkoxy C–O stretching	1104	1095
Aromatic C–H bending	786	777
Alkyl C–Br stretching	518	516

$$M_{\text{ad}} = \frac{Q_d C_w}{q_{\text{ad}}} \int_0^{t_R} \left(1 - \frac{C_t}{C_w}\right) dt \quad (11)$$

where  $t_R$  corresponds to the value of  $C_t$  which is less than  $C_d$  or equal to  $C_d$  and  $C_t$  is taken from the experimental data. The height of the proposed setup is determined using the below equation,

$$H = H_c + \frac{4M_{\text{ad}}}{\pi v D^2} \quad (12)$$

In this study, Thomas model is fitted well with best correlation coefficient 0.9935. The specification for the pump, glass column, and other accessories should be added to the industrial design. Therefore, the laboratory-scale data should be readjusted to construct an exact design in industrial scale.

### FTIR study

Fourier transform infrared spectroscopy (FTIR) is a mechanism which is used to collect an infrared spectrum of absorption of the adsorbent. It is an easy technique to identify the presence of functional groups in a molecule. Figure 3 refers to the FTIR diagram for fresh and Cr(VI) loaded of guava leaf. The shift in wavelength is noticed in the figure. The figure indicates the shift in wave number from 4000 to 400  $\text{cm}^{-1}$  for metal ion unloaded and metal ion-loaded guava leaves which are represented in Table 4. The responsibility of Alkyl C–H stretching is identified from the shifting in wave number from 2931 (unloaded adsorbent) to 2927  $\text{cm}^{-1}$  [Cr(VI) ion-loaded adsorbent]. Aromatic C=C bending is also responsible for the adsorption as the peak in wavelength is shifted from 1623 (unloaded adsorbent) to 1619  $\text{cm}^{-1}$  [Cr(VI) ion-loaded adsorbent]. The shift from 1456 (unloaded adsorbent) to 1445  $\text{cm}^{-1}$  [Cr(VI) ion-loaded adsorbent] indicated the carboxylate anion C=O is stretching, and –SO<sub>3</sub> stretching is indicated by the shift from 1240 (unloaded adsorbent) to 1236  $\text{cm}^{-1}$  [Cr(VI) ion-loaded adsorbent]. Alkoxy C–O stretching is also responsible for

the respective adsorption as the wave number is shifted from 1104 (unloaded adsorbent) to 1095  $\text{cm}^{-1}$  (metal-loaded adsorbent). The shifting in wave number from 786 (unloaded adsorbent) to 777  $\text{cm}^{-1}$  (metal-loaded adsorbent) and 518 (unloaded adsorbent) to 516  $\text{cm}^{-1}$  (metal-loaded adsorbent) is due to the Alkyl C–Br stretching and aromatic C–H bending; hence, they are also responsible in the metal binding adsorption process.

### Conclusions

It is concluded that the guava leaves are capable of adsorbed metal ions in continuous mode. The operating factors like bed depth, flow rate, and influent concentration of metal ion affect the adsorption capacity and breakthrough profiles. Adsorption was best at high bed depth but low rate of flow and influent concentration. Among Thomas and Bohart–Adams models, Thomas model was the best kinetic model. From the FTIR study, the functional groups like alkyl C–H are stretching, aromatic C=C bending, carboxylate anion C=O stretching, SO<sub>3</sub> stretching, alkoxy C–O stretching, alkyl C–Br stretching, and aromatic C–H bending was identified as Cr(VI) adsorption. From the mass transfer zone determination, it was established that the total amount of adsorbent in the bed is not used for the sorption process. The scale-up design procedure is described. The guava leaves are useful adsorbent and suitable for Third World countries for removal of Cr(VI) ions.

**Acknowledgements** Authors are thankful to DST, Government of West Bengal for the project [Sanction order No. 211(Sanc.)/ST/P/S&T/13G-1/2013, dated–06.06.2014]. T. Mitra is thankful to TEQIP Phase-II [Ref. No. TEQIP-II/ACA/86 (4/2), dated 18.09.2013], University of Calcutta for her fellowship.

### Compliance with ethical standards

**Conflict of interest** No conflict of interest is confirmed.

**Open Access** This article is distributed under the terms of the Creative Commons Attribution 4.0 International License (<http://creativecommons.org/licenses/by/4.0/>), which permits unrestricted use, distribution, and reproduction in any medium, provided you give appropriate credit to the original author(s) and the source, provide a link to the Creative Commons license, and indicate if changes were made.

### References

- Agarwal GS, Bhuptawat HK, Chaudhari S (2006) Biosorption of aqueous chromium (VI) by *Tamarindus indica* seeds. *Bioresour Technol* 97:949
- Alguacil FJ, Alonso M, Lopez F, Lopez-Delgado A (2008) Uphill permeation of Cr(VI) using Hostarex A327 as ionophore by membrane-solvent extraction processing. *Chemosphere* 72:684

- Bohart G, Adams EN (1920) Some aspects of the behavior of charcoal with respect to chlorine. *J Am Chem Soc* 42:523
- Dakiky M, Khami A, Manassra A, Mer'eb M (2002) Selective adsorption of chromium (VI) in industrial wastewater using low-cost abundantly available adsorbents. *Adv Environ Res* 6(4):533
- EPA (1990) Environmental Protection Agency, Cincinnati OH USA
- Geankoplis CJ (2016) Transport processes and separation processes principles, 4th edn. Prentice-Hall of India Pvt. Ltd., New Delhi, India
- Hossen SM (2012) Statistical analysis of current guava production and its prospect in Bangladesh. *Asian Bus Rev* 1(1):9
- IS 10500:1991 (1991) Bureau of Indian standards, Drinking Water Specifications, New Delhi
- Kalavathy H, Karthik B, Miranda LR (2010) Removal and recovery of Ni and Zn from aqueous solution using activated carbon from *Hevea brasiliensis*: batch and column studies. *Colloids Surf B Biointerfaces* 78:291
- Kalhari EM, Yetilmezsoy K, Uygur N, Zarrabi M, Abu Shmeis RM (2013) Modeling of adsorption of toxic chromium on natural and surface modified lightweight expanded clay aggregate (LECA). *Appl Surf Sci* 287:428
- Kyzas GZ, Kostoglou M (2014) Green adsorbents for wastewaters: a critical review. *Materials* 7:333
- Long Y, Lei D, Ni J, Ren Z, Chen C, Xu H (2014) Packed bed column studies on lead(II) removal from industrial wastewater by modified *Agaricus bisporus*. *Bioresour Technol* 152:457
- Malkoc E, Nuhoglu Y, Dundar M (2006) Adsorption of chromium(VI) on pomace—an olive oil industry waste: batch and column study. *J Hazard Mater B* 138:142
- Mitra T, Das SK (2016) Adsorptive removal of Cr(VI) from aqueous solution using blackberry leaves—column study. *Int J Environ Eng* 8(4):225
- Mitra T, Singha B, Bar N, Das SK (2014) Removal of Pb(II) ions from aqueous solution using water hyacinth root by fixed-bed column and ANN modelling. *J Hazard Mater* 273:94
- Mondal MK (2009) Removal of Pb(II) ions from aqueous solution using activated tea waste: adsorption on a fixed-bed column. *J Environ Manage* 90:3266
- Nag S, Mondal A, Bar N, Das SK (2017) Biosorption of chromium (VI) from aqueous solutions and ANN modelling. *Environ Sci Pollut Res* 24(23):18817
- Quintelas C, Fonseca B, Silva B, Figueiredo H, Tavares T (2009) Treatment of chromium(VI) solutions in a pilot-scale bioreactor through a biofilm of *Arthrobacter viscosus* supported on GAC. *Bioresour Technol* 100:220
- Setshedi KZ, Bhaumik M, Onyango MS, Maity A (2015) High-performance towards Cr(VI) removal using multi-active sites of polypyrrole–graphene oxide nanocomposites: batch and column studies. *Chem Eng J* 262:921
- Shruthi SD, Roshan A, Timilsina SS, Sunita S (2013) A review on the medicinal plant *Psidium guajava* Linn. (Myrtaceae). *J Drug Deliv Ther* 3(2):162
- Singha B, Naiya TK, Bhattacharya AK, Das SK (2011) Cr(VI) ions removal from aqueous solutions using natural adsorbents—FTIR studies. *J Environ Prot* 2:729
- Sousa FW, Oliveira AG, Ribeiro JP, Rosa MF, Keukeleire D, Nascimento RF (2010) Green coconut shells applied as adsorbent for removal of toxic metal ions using fixed-bed column technology. *J Environ Manage* 91:1634
- Talreja N, Kumar D, Verma N (2014) Removal of hexavalent chromium from water using Fe-grown carbon nanofibers containing porous carbon microbeads. *J Water Proc Eng* 3:34
- Thomas HG (1948) Chromatography: a problem in kinetics. *Ann N Y Acad Sci* 49:161
- Uguzdogan E, Denkbaz EB, Kabasakal OS (2010) The use of poly-ethyleneglycolmethacrylate-co-vinylimidazole (PEGMA-co-VI) micro-spheres for the removal of nickel(II) and chromium(VI) ions. *J Hazard Mater* 177:119
- WHO (1993) Guidelines for drinking water quality, vol 1. World Health Organization, Geneva, p 52
- Ye J, Yin H, Mai B, Peng H, Qin H, He B, Zhang N (2010) Biosorption of chromium from aqueous solution and electroplating wastewater using mixture of *Candida lipolytica* and dewatered sewage sludge. *Bioresour Technol* 101:3893

**Publisher's Note** Springer Nature remains neutral with regard to jurisdictional claims in published maps and institutional affiliations.